

# Syndiotactic Polystyrene Aerogels: Adsorption in Amorphous Pores and Absorption in Crystalline Nanocavities

Christophe Daniel,<sup>\*,†</sup> Diana Sannino,<sup>‡</sup> and Gaetano Guerra<sup>†</sup>

Dipartimento di Chimica, Università di Salerno, Via Ponte Don Melillo, 84084 Fisciano (SA), Italy, and  
Dipartimento di Ingegneria Chimica ed Alimentare, Università di Salerno, Via Ponte Don Melillo,  
84084 Fisciano (SA), Italy

Received August 30, 2007. Revised Manuscript Received November 2, 2007

Sorption experiments have been conducted for syndiotactic polystyrene (s-PS) aerogels with different crystalline forms and of different porosities. Nitrogen uptake experiments at 77 K have confirmed that  $\delta$ -form aerogels present crystalline nanocavities as well as amorphous porosity. The equilibrium uptake of organic molecules, from dilute aqueous solutions, for  $\delta$ -form aerogels is high (e.g., more than 5 wt % of 1,2-dichloroethane, DCE, from 1 ppm solutions) and independent of aerogel porosity. Gravimetric experiments, as well as FTIR conformational studies on absorbed DCE, clearly indicate that guest absorption from diluted solutions occurs only in the crystalline nanocavities. High-porosity  $\delta$ -form aerogels ( $P > 98\%$ ) can also exhibit substantial water adsorption from the amorphous porosity, which is favorable to the pollutant absorption kinetics. In fact, apparent guest diffusivity increases of several orders of magnitude, with respect to the corresponding films, have been observed.

## Introduction

Syndiotactic polystyrene (s-PS) presents a complex poly-morphic behavior mainly based on four crystalline forms (named  $\alpha$ ,  $\beta$ ,  $\gamma$ , and  $\delta$ ).<sup>1,2</sup> In addition, s-PS is able to cocrystallize with several low-molecular-mass compounds

leading to cocrystals (clathrate<sup>3</sup> and intercalate<sup>4</sup>), which by using suitable guests have been proposed as advanced optical materials.<sup>5</sup>

The  $\delta$ -form<sup>2</sup> (also called emptied  $\delta$ -form in previous reports<sup>2a,b,6a</sup>), whose crystal structure has been fully described,<sup>2b,d</sup> can be obtained by complete guest removal from cocrystals, by suitable extraction procedures.<sup>2b,c</sup> The  $\delta$ -form is characterized by the presence of two cavities per unit cell (whose volume is close to 0.12 nm<sup>3</sup>)<sup>2b,d</sup> and is able to rapidly absorb volatile organic compounds (VOCs) (mainly halogenated or aromatic hydrocarbons) from water and air, also when present at very low concentrations.<sup>6</sup> Moreover, these materials are hydrophobic and hence seem particularly suitable for applications in chemical separation, in water and moist air purification,<sup>6a,d</sup> and in sensors.<sup>7</sup>

It is also well-known that the diffusion kinetics of volatile organic compounds are strongly dependent on the morphology of the semicrystalline materials. In particular, fine powders present fast diffusion kinetics but are difficult to handle. On the other hand, morphologies with small surface

\* Corresponding author. E-mail: cdaniel@unisa.it.

<sup>†</sup> Dipartimento di Chimica.

<sup>‡</sup> Dipartimento di Ingegneria Chimica ed Alimentare.

- (1) (a) Guerra, G.; Vitagliano, V. M.; De Rosa, C.; Petraccone, V.; Corradini, P. *Macromolecules* **1990**, *23*, 1539–1544. (b) Chatani, Y.; Shimane, Y.; Inoue, Y.; Inagaki, T.; Ishioka, T.; Ijitsu, T.; Yukinari, T. *Polymer* **1992**, *33*, 488–492. (c) Rizzo, P.; Albulia, A. R.; Guerra, G. *Polymer* **2005**, *46*, 9549–9554.
- (2) (a) Manfredi, C.; DeRosa, C.; Guerra, G.; Rapacciuolo, M.; Auriemma, F.; Corradini, P. *Macromol. Chem. Phys.* **1995**, *196*, 2795–2808. (b) De Rosa, C.; Guerra, G.; Petraccone, V.; Pirozzi, B. *Macromolecules* **1997**, *30*, 4147–4152. (c) Reverchon, E.; Guerra, G.; Venditto, V. *J. Appl. Polym. Sci.* **1999**, *74*, 2077–2082. (d) Milano, G.; Venditto, V.; Guerra, G.; Cavallo, L.; Ciambelli, P.; Sannino, D. *Chem. Mater.* **2001**, *13*, 1506–1511. (e) Gowd, E. B.; Shibayama, N.; Tashiro, K. *Macromolecules* **2006**, *39*, 8412–8418.
- (3) (a) Immirzi, A.; de Candia, F.; Iannelli, P.; Zambelli, A.; Vittoria, V. *Makromol. Chem., Rapid Commun.* **1988**, *9*, 761–764. (b) Chatani, Y.; Shimane, Y.; Inagaki, T.; Ijitsu, T.; Yukimori, T.; Shikuma, H. *Polymer* **1993**, *34*, 1620–1624. (c) Chatani, Y.; Inagaki, T.; Shimane, Y.; Shikuma, H. *Polymer* **1993**, *34*, 4841–4845. (d) De Rosa, C.; Rizzo, P.; Ruiz de Ballesteros, O.; Petraccone, V.; Guerra, G. *Polymer* **1999**, *40*, 2103–2110. (e) Tarallo, O.; Petraccone, V. *Macromol. Chem. Phys.* **2004**, *205*, 1351–1360. (f) Tarallo, O.; Petraccone, V. *Macromol. Chem. Phys.* **2005**, *206*, 672–679. (g) Kaneko, F.; Uda, Y.; Kajivara, A.; Tanigaki, N. *Macromol. Rapid Commun.* **2006**, *27*, 1643–1647.
- (4) (a) Petraccone, V.; Tarallo, O.; Venditto, V.; Guerra, G. *Macromolecules* **2005**, *38*, 6965–6971. (b) Tarallo, O.; Petraccone, V.; Venditto, V.; Guerra, G. *Polymer* **2006**, *47*, 2402–2410. (c) Malik, S.; Rochas, C.; Guenet, J. M. *Macromolecules* **2006**, *39*, 1000–1007. (d) Galdi, N.; Albulia, A. R.; Oliva, L.; Guerra, G. *Macromolecules* **2006**, *39*, 9171–9176.
- (5) (a) Venditto, V.; Milano, G.; De Girolamo Del Mauro, A.; Guerra, G.; Mochizuki, J.; Itagaki, H. *Macromolecules* **2005**, *38*, 3696–3702. (b) Stegmaier, P.; De Girolamo Del Mauro, A.; Venditto, V.; Guerra, G. *Adv. Mater.* **2005**, *17*, 1166–1168. (c) Uda, Y.; Kaneko, F.; Tanigaki, N.; Kawaguchi, T. *Adv. Mater.* **2005**, *17*, 1846–1850. (d) D'Aniello, C.; Musto, P.; Venditto, V.; Guerra, G. *J. Mater. Chem.* **2007**, *17*, 531–535. (e) Daniel, C.; Galdi, N.; Montefusco, T.; Guerra, G. *Chem. Mater.* **2007**, *19*, 3302–3308.

- (6) (a) Manfredi, C.; Del Nobile, M. A.; Mensitieri, G.; Guerra, G.; Rapacciuolo, M. *J. Polym. Sci., Polym. Phys. Ed.* **1997**, *35*, 133–140. (b) Musto, P.; Mensitieri, G.; Cotugno, S.; Guerra, G.; Venditto, V. *Macromolecules* **2002**, *35*, 2296–2304. (c) Mahesh, K. P. O.; Tsujita, Y.; Yoshimizu, H.; Okamoto, S.; Mohan, D. *J. Polym. Sci., Part B: Polym. Phys.* **2005**, *43*, 2380–2387. (d) Venditto, V.; De Girolamo Del Mauro, A.; Mensitieri, G.; Milano, G.; Musto, P.; Rizzo, P.; Guerra, G. *Chem. Mater.* **2006**, *18*, 2205–2210. (e) Malik, S.; Roizard, D.; Guenet, J. M. *Macromolecules* **2006**, *39*, 5957–5959.
- (7) (a) Mensitieri, G.; Venditto, V.; Guerra, G. *Sens. Actuators, B* **2003**, *92*, 255–261. (b) Giordano, M.; Russo, M.; Cusano, A.; Cutolo, A.; Mensitieri, G.; Nicolais, L. *Appl. Phys. Lett.* **2004**, *85*, 5349–5351. (c) Giordano, M.; Russo, M.; Cusano, A.; Mensitieri, G.; Guerra, G. *Sens. Actuators, B* **2005**, *109*, 177–184. (d) Cusano, A.; Pilla, P.; Contessa, L.; Iadicicco, A.; Campopiano, S.; Cutolo, A.; Giordano, M.; Guerra, G. *Appl. Phys. Lett.* **2005**, *87*, 234105/1–234105/3.

area (film, sheet) are easier to handle for uses in molecular separation processes, but they display much slower diffusion kinetics.

Recently, it has been shown that high-porosity s-PS aerogels can be obtained by supercritical CO<sub>2</sub> extraction of the solvent present in s-PS physical gels<sup>8a,b</sup> or by sublimation of the solvent.<sup>8c,d</sup> The crystalline phase of the aerogels and their structure depend on the crystalline structure (cocrystalline or  $\beta$ ) of the junction zones of the starting gel.<sup>8a,b</sup> When the polymer-rich phase of the gel is a cocrystal, the corresponding aerogel is formed by semicrystalline nanofibrils (fibril diameter range between 100 and 200 nm) exhibiting the nanoporous crystalline  $\delta$ -phase while when the crystalline phase of the gel is the  $\beta$ -phase, the corresponding aerogel is characterized by  $\beta$ -phase<sup>9</sup> interconnected lamellar crystals (thickness in the range 200–400 nm).<sup>8a,b</sup>

Chloroform-vapor sorption measurements at low chloroform pressure have shown that  $\delta$ -form aerogels exhibit the high sorption capacity characteristic of s-PS  $\delta$ -form samples (due to the sorption of molecules as isolated guests of the host nanoporous crystalline phase) associated with the high sorption kinetics typical for aerogels (due to the high porosity and hence high surface area).<sup>8a,b</sup> Thus, these new materials present fast sorption kinetics while maintaining convenient handling characteristics.

In order to better characterize the sorption capacity and kinetics of s-PS aerogels and to assess possible uses of this new material, sorption measurements of nitrogen (at 77 K) and of diluted organic compounds from their aqueous solutions (at room temperature) have been conducted.

## Experimental Section

**Materials.** The syndiotactic polystyrene used in this study was manufactured by Dow Chemicals under the trademark Questra 101. <sup>13</sup>C nuclear magnetic resonance characterization showed that the content of syndiotactic triads was over 98%. The mass average molar mass obtained by gel permeation chromatography (GPC) in trichlorobenzene at 135 °C was found to be  $M_w = 3.2 \times 10^5$  g mol<sup>-1</sup> with a polydispersity index  $M_w/M_n = 3.9$ . Solvents used to prepare the gels were purchased from Aldrich and used without further purification.

All s-PS gel samples were prepared in hermetically sealed test tubes by heating the mixtures above the boiling point of the solvent until complete dissolution of the polymer, and the appearance of a transparent and homogeneous solution had occurred. Then the hot solution was cooled to room temperature where gelation occurred.

$\delta$  and  $\beta$  aerogel samples were obtained by treating sPS/toluene and sPS/chlorotetradecane native gels, respectively, with a SFX 200 supercritical carbon dioxide extractor (ISCO Inc.) using the following conditions:  $T = 40$  °C,  $P = 200$  bar, extraction time  $t = 60$  min.

The  $\gamma$ -form s-PS aerogels, not yet described in the literature, were obtained by treating sPS/1,2-dichloroethane gels using the

following CO<sub>2</sub> extractor conditions:  $T = 125$  °C,  $P = 310$  bar, extraction time  $t = 90$  min.

The degree of crystallinity of the aerogels and powder samples was evaluated from X-ray diffraction data applying the standard procedure of resolving the diffraction pattern into two areas corresponding to the contributions of the crystalline and amorphous fractions. In particular, the degree of crystallinity of the  $\delta$ - and  $\gamma$ -powders is close to 35% while for the  $\beta$ -,  $\gamma$ -, and  $\delta$ -aerogels it is close to 48%, 45%, and 40%, respectively. For  $\delta$ -form film samples, the degree of crystallinity measured by the FTIR method, which has been described for trans-planar<sup>9</sup> and helical<sup>6b,10</sup> crystalline phases, is in the range 35–40%.

The porosity  $P$  of aerogel samples can be expressed as a function of the aerogel apparent density  $\rho$  as

$$P = 100 \times \left( 1 - \frac{\rho}{\rho_s} \right) \quad (1)$$

where  $\rho_s$  is the density of the polymer matrix (equal to 1.02 g/cm<sup>3</sup>, for a semicrystalline  $\delta$ -form s-PS with a crystallinity of nearly 40%).

**Techniques.** Nitrogen adsorption experiments were conducted by a Thermoquest Sorptomatic 1990. Powder and aerogel samples were outgassed ( $10^{-4}$  Torr) at ambient temperature. For specific surface area calculation, the two-parameter BET method in the range 0.05–0.30  $p/p^0$  was used.

Aerogel equilibrium sorption isotherms, sorption and desorption kinetics with aqueous solutions were obtained by measurements of FTIR absorbances of conformationally sensitive peaks of 1,2-dichloroethane (DCE),<sup>11</sup> by using calibration curves analogous to those described in ref 11a,e,g.

Infrared spectra were obtained at a resolution of 2.0 cm<sup>-1</sup> with a Vector 22 Bruker spectrometer equipped with deuterated triglycine sulfate (DTGS) detector and a KBr beam splitter. The frequency scale was internally calibrated to 0.01 cm<sup>-1</sup> using a He–Ne laser. Eight scans were signal averaged to reduce the noise.

Aerogel equilibrium sorption isotherms and desorption kinetics with aqueous solutions were also obtained by gravimetric measurements. The weight gain of samples was determined with a TG50 Mettler analytical balance (0.01 mg precision) after wiping of the aerogels.

## Results and Discussion

**Nitrogen Sorption.** Following a standard procedure for porosity evaluation of powders,<sup>12</sup> nitrogen sorption experiments at low temperature (77 K) were conducted with  $\delta$ -aerogels with a porosity  $P = 91\%$  and  $P = 98.5\%$  and  $\beta$ -aerogel with  $P = 91\%$ .

Sorption isotherms in the range 0–0.30  $p/p_0$  of  $\delta$ - and  $\beta$ -aerogels (filled symbols) are compared with the sorption isotherms of  $\delta$ - and  $\gamma$ -powders (70–100 mesh size, empty

- (8) (a) Daniel, C.; Alfano, D.; Venditto, V.; Cardea, S.; Reverchon, E.; Larobina, D.; Mensitieri, G.; Guerra, G. *Adv. Mater.* **2005**, *17*, 1515–1518. (b) Guerra, G.; Mensitieri, G.; Venditto, V.; Reverchon, E.; Daniel, C. PCT Int. Appl. WO 2005012402, 2005. (c) Malik, S.; Rochas, C.; Guenet, J.-M. *Macromolecules* **2005**, *38*, 4888–4893. (d) Malik, S.; Roizard, D.; Guenet, J.-M. *Macromolecules* **2006**, *39*, 5957–5959. (9) Musto, P.; Tavone, S.; Guerra, G.; De Rosa, C. *J. Polym. Sci., Polym. Phys.* **1997**, *35*, 1055–1066.

- (10) Albulia, A. R.; Musto, P.; Guerra, G. *Polymer* **2006**, *47*, 234–242. (11) (a) Guerra, G.; Manfredi, C.; Musto, P.; Tavone, S. *Macromolecules* **1998**, *31*, 1329–1334. (b) Musto, P.; Manzari, M.; Guerra, G. *Macromolecules* **1999**, *32*, 2770–2776. (c) Musto, P.; Manzari, M.; Guerra, G. *Macromolecules* **2000**, *33*, 143–149. (d) Guerra, G.; Milano, G.; Venditto, V.; Musto, P.; De Rosa, C.; Cavallo, L. *Chem. Mater.* **2000**, *12*, 363–368. (e) Daniel, C.; Musto, P.; Guerra, G. *Macromolecules* **2002**, *35*, 2243–2251. (f) Daniel, C.; Alfano, D.; Guerra, G.; Musto, P. *Macromolecules* **2003**, *36*, 1713–1716. (g) Daniel, C.; Alfano, D.; Guerra, G.; Musto, P. *Macromolecules* **2003**, *36*, 5742–5750. (h) Musto, P.; Rizzo, P.; Guerra, G. *Macromolecules* **2005**, *38*, 6079–6089. (12) Gregg, S. J.; Sing, K. S. W. In *Adsorption, Surface Area and Porosity*; Academic Press: London, 1982.

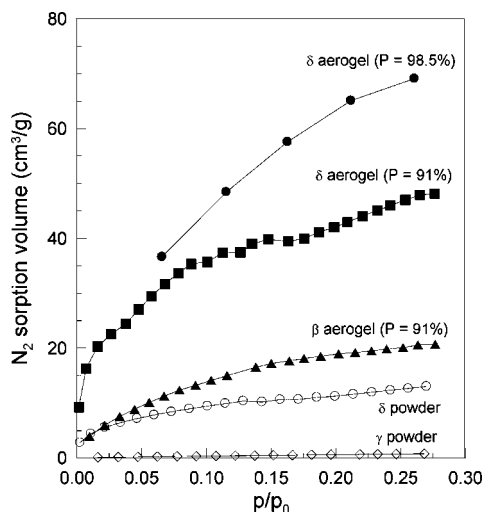


**Figure 1.** Nitrogen sorption isotherms in the range 0–0.30  $p/p_0$  of  $\delta$ -aerogels ( $P = 91\%$  and  $98.5\%$ ),  $\beta$ -aerogel ( $P = 91\%$ ),  $\delta$ -powder, and  $\gamma$ -powder at 77 K. The sorption is expressed as  $\text{cm}^3$  of nitrogen in normal conditions (1 atm, 273 K) per gram of polymer.

**Table 1.** Nitrogen Sorption and BET Values As Derived by Isotherm Curves of Figure 1

s-PS sample	$\text{N}_2$ sorption at $p/p^0 = 0.1$ ( $\text{cm}^3/\text{g}$ )	BET <sup>a</sup> ( $\text{m}^2/\text{g}$ )
$\gamma$ -powder	0.3	4
$\delta$ -powder	9	43
$\beta$ -aerogel ( $P = 91\%$ )	14	70
$\delta$ -aerogel ( $P = 91\%$ )	35	157
$\delta$ -aerogel ( $P = 98.5\%$ )	45	260

<sup>a</sup> As evaluated in the range 0.05–0.30  $p/p^0$ .

symbols)<sup>2d</sup> in Figure 1, where the sorption is expressed as  $\text{cm}^3$  of nitrogen in normal conditions (1 atm, 0 °C) per gram of polymer.

The sorption curves of Figure 1 and relevant data derived from them (Table 1) show that the sorption capacity is markedly larger for samples presenting the crystalline nanocavities of the  $\delta$ -phase, and it also markedly increases with the porosity of the amorphous phase.

As discussed in detail in ref 2d, the nitrogen sorption observed with dense s-PS samples (powder or films) is nearly entirely due to its inclusion as guest into the nanocavities of the  $\delta$ -crystalline phase. In this respect it is worth adding that recent gravimetric, X-ray diffraction, and infrared linear dichroism studies, relative to gas sorption in nanoporous s-PS  $\delta$ -phases,<sup>13</sup> have shown the formation of real s-PS/gas clathrate phases with carbon dioxide and butadiene.<sup>13b</sup>

With reference to the sorption curves of Figure 1, it is also worth noting that the sum of nitrogen uptake from  $\delta$ -powder (empty circles, corresponding to absorption only in the crystalline nanocavities<sup>2c,8</sup>) and  $\beta$ -aerogel (triangles) is comparable with the nitrogen uptake from the  $\delta$ -aerogel of equal porosity (filled squares). Nitrogen uptake from  $\beta$ -aerogels, due to the negligible empty volume<sup>2d</sup> and guest uptake<sup>14</sup> from its high density ( $1.078 \text{ g/cm}^3$ )  $\beta$ -crystalline phase,<sup>15</sup> is entirely due to adsorption on the amorphous porosity. This clearly indicates that  $\delta$ -aerogels, beside the

(13) (a) Larobina, D.; Sanguigno, L.; Venditto, V.; Guerra, G.; Mensitieri, G. *Polymer* **2004**, *45*, 429–436. (b) Annunziata, L.; Albonia, A. R.; Venditto, V.; Mensitieri, G.; Guerra, G. *Macromolecules* **2006**, *39*, 9166–9170.

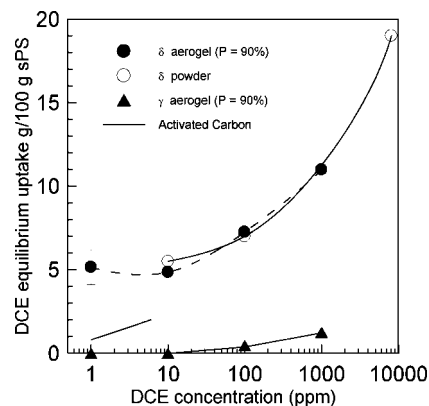


**Figure 2.** Equilibrium DCE sorption at room temperature by  $\delta$ -aerogel ( $P = 90\%$ , filled circles),  $\delta$ -powder (empty circles), and  $\gamma$ -aerogels ( $P = 90\%$ , triangles) as determined by FTIR measurements. For the sake of comparison DCE sorption from activated carbon is also reported (thin line, data from ref 17).

usual nitrogen *absorption* into the crystalline nanocavities, present a substantial nitrogen *adsorption* on the large surface area of the amorphous porosity.

The curves of Figure 1 also show that the increments of nitrogen uptake, which are observed when we compare  $\delta$ -powder and  $\delta$ -aerogels, increase with aerogel porosity. This confirms the previous conclusion that the increment of nitrogen uptake of aerogels with respect to the powder is due to adsorption in the amorphous pores.

**Sorption of Organic Molecules from Dilute Aqueous Solutions.** The equilibrium uptake of DCE from diluted aqueous solutions has been investigated for several s-PS samples. The choice of DCE was motivated by the additional information, which comes from its conformational equilibrium. In fact, as described in detail in previous papers,<sup>11</sup> since essentially only its trans conformer is included into the clathrate phase while both trans and gauche conformers are included in the amorphous phase, quantitative evaluations of vibrational peaks associated with these conformers allow us to evaluate the amounts of DCE confined as guest in the clathrate phase or simply absorbed in the amorphous phase. The choice of DCE was also motivated by its presence in contaminated aquifers and by its resistance to remediation techniques based on reactive barriers containing Fe.<sup>16</sup>

DCE equilibrium uptakes from diluted aqueous solutions from  $\gamma$  aerogel ( $P = 90\%$ ),  $\delta$ -aerogel ( $P = 90\%$ ), and  $\delta$ -powder, as obtained by FTIR measurements, are compared in Figure 2. For the sake of comparison, the equilibrium sorption capacity of DCE from activated carbon is also shown.<sup>17</sup>

(14) (a) Guerra, G.; Vitagliano, V. M.; Corradini, P.; Albizzati, E. *It Pat* 19588 (Himont Inc.), 1989. (b) Vittoria, V.; Russo, R.; de Candia, F. *J. Macromol. Sci., Phys.* **1989**, *B28*, 419–431. (c) Rapacciuolo, M.; De Rosa, C.; Guerra, G.; Mensitieri, G.; Apicella, A.; Del Nobile, M. A. *J. Mater. Sci. Lett.* **1991**, *10*, 1084–1087.

(15) (a) De Rosa, C.; Rapacciuolo, M.; Guerra, G.; Petraccone, V.; Corradini, P. *Polymer* **1992**, *33*, 1423–1428. (b) Chatani, Y.; Shimane, Y.; Ijitsu, T.; Yukinari, T. *Polymer* **1993**, *34*, 1625–1629.

(16) (a) Di Molfetta, A.; Sethi, R. *Environ. Geol.* **2006**, *50*, 361–369. (b) Jeen, S.-W.; Jambor, J. L.; Blowes, D. W.; Gillham, R. W. *Environ. Sci. Technol.* **2007**, *41*, 1989–1994.

(17) Stanzel, M. H. *Chem. Eng. Prog.* **1993**, *89* (4), 36–43.



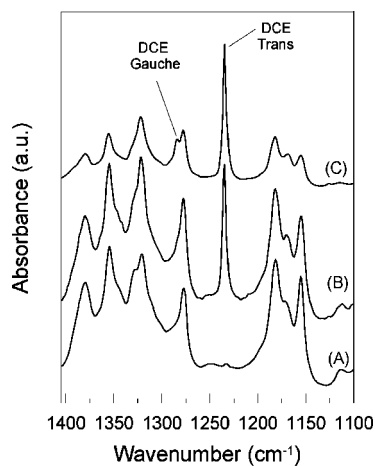


**Figure 3.** FTIR spectra of a  $\delta$ -aerogel with  $P = 90\%$  before (A) and after equilibrium DCE sorption from its aqueous 1 ppm (B) and 1000 ppm (C) solutions.

The VOC uptake of  $\delta$ -form powder and aerogels are almost identical, as also confirmed by measurements on aerogels with porosity in the range 98.5–80% (not reported in Figure 2). Particularly relevant are the results relative to the VOC uptake from the most diluted aqueous solution (1 ppm) showing that the sorption capacity is larger than  $5 \text{ g}_{\text{DCE}}/100 \text{ g}_{\text{polymer}}$ , i.e., leading to a concentration increase of 50 000 times.

Moreover, it is clearly apparent that the DCE uptake from the  $\gamma$  aerogel is always much lower than for the  $\delta$ -form samples and becomes negligible for dilute aqueous solutions. This clearly indicates that the DCE uptake occurs essentially only in the crystalline nanoporous phase.

As mentioned above, the fraction of DCE absorbed in the nanoporous crystalline phase and in the amorphous phase of the aerogels can be quantitatively estimated from the conformational equilibrium of DCE molecules, as established by FTIR measurements.

In particular, the FTIR spectra of a  $\delta$ -aerogel with porosity  $P = 90\%$ , before (curve A) and after DCE equilibrium sorption from aqueous 1 ppm (curve B) and 1000 ppm (curve C) solutions, are reported in Figure 3.

We can observe that, by decreasing the DCE concentration in the solution, the absorbance of the gauche DCE peak at  $1284 \text{ cm}^{-1}$  becomes negligible.<sup>18</sup> From the absorbance of the trans and gauche peaks (by considering that the conformer molar fraction of trans DCE molecules absorbed in the nanoporous crystalline phase and in the amorphous phase is 0.94 and 0.51, respectively),<sup>11</sup> it is possible to calculate that, after equilibrium sorption from 1000 and 1 ppm solutions, nearly 80% and 100% of the DCE molecules absorbed by the  $\delta$ -aerogels is located in the crystalline phase.

**Guest Diffusion Kinetics.** DCE sorption kinetics of  $\delta$ -form aerogels with a porosity  $P = 98.5\%$ , 90%, and 80% from 100 ppm (A) and 10 ppm (B) solutions, as obtained by FTIR measurements, are compared in Figure 4. DCE desorption experiments at room temperature in air, from

aerogels with  $P = 98.5\%$ ,  $P = 90\%$ , and  $P = 80\%$ , after equilibrium absorption from 100 ppm aqueous solution, are reported in Figure 5. For the sake of comparison, the desorption kinetics for a film, having a thickness of nearly  $40 \mu\text{m}$ ,<sup>6d</sup> is also reported as the inset in Figure 5.

As in previous papers,<sup>6b,2d,13a</sup> the DCE uptake is reported versus square root of time divided by the aerogel macroscopic thickness, to put in evidence Fick's sorption behavior. The apparent diffusivities ( $D$ ) as evaluated from line slopes have been collected in Table 2.

We can clearly observe a significant increase of the apparent diffusivity with the aerogel porosity (i.e., specific surface area). In particular, for a 100 ppm DCE aqueous solution, the diffusivity constant of a 98.5% porosity aerogel is ca. 60 times larger than for a 90% porosity aerogel and ca. 120 times larger than for a 80% aerogel.

Moreover, this increase of diffusivity constant with porosity appears to be more pronounced when the VOC concentration in the aqueous solution is reduced, and for a 10 ppm DCE aqueous solution the diffusivity constant of the 98.5% porosity aerogel is more than 250 times larger than for a 90% porosity aerogel. For this low DCE concentration, sorption in the 98.5% porosity aerogel (1 mm thickness) reaches the equilibrium DCE uptake after ca. 30 min, when the 90% porosity aerogel has absorbed less than 10% of its equilibrium uptake.

The diffusivity constants of the aerogels are much higher than those obtained for films. In particular, the diffusivity of a  $\delta$ -aerogel with  $P = 98.5\%$  in a 100 ppm DCE aqueous solution is nearly 7 orders of magnitude larger than the diffusivity constant obtained for  $\delta$ -form films.<sup>6d</sup> Of course, the higher apparent diffusivities observed with aerogels are due to their higher specific surface area.

With reference to the sorption kinetics of Figure 4, it is also worth adding that mainly for the aerogels of lower porosity ( $P < 90\%$ ) the sorption is slower for short times and reaches the final linear Fickian behavior only after a sorption time, which increases as the VOC concentration decreases. This phenomenon is possibly due to the presence of a skin of lower permeability, as often observed for polymer foams,<sup>19</sup> which affects guest sorption mainly for low-porosity aerogels.

As for the desorption experiments, the diffusivities are smaller than those of the corresponding sorption experiments, as already observed for  $\delta$ -form films.<sup>6b</sup> It is also worth noting that, after 3000 h of desorption, nearly 2 wt % of DCE (nearly 40% of the initial content) is still present in the polymer film while complete DCE desorption occurs in ca. 50 and 10 h for aerogels with 80% and 98.5% porosity, respectively.

**Water Adsorption in High-Porosity  $\delta$ -Aerogels.** The desorption kinetics obtained from gravimetric measurements of aerogels with porosity  $P = 90.5\%$  and  $P = 98.5\%$ , after equilibrium sorption in 100 ppm aqueous solution of DCE, are compared in Figure 6.

(18) (a) Tanabe, K. *Spectrochim. Acta* **1972**, *28A*, 407–424. (b) Alburnia, A. R.; Di Masi, S.; Rizzo, P.; Milano, G.; Musto, P.; Guerra, G. *Macromolecules* **2003**, *36*, 8695–8703.

(19) (a) Abdul-Rani, A. M.; Hopkinson, N.; Dickens, P. M. *J. Cell. Plast.* **2005**, *41*, 133–151. (b) Blanchet, J. F.; Rodrigue, D. *Cell. Polym.* **2004**, *23*, 193–210.

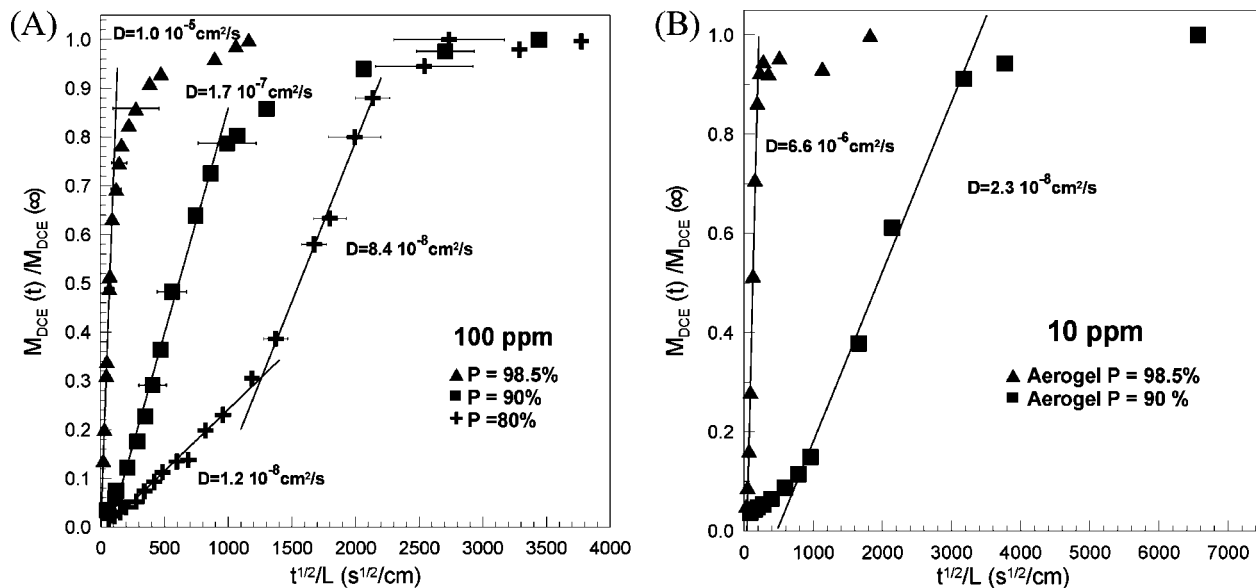


**Figure 4.** Sorption kinetics at room temperature of DCE from 100 ppm (A) and 10 ppm (B) DCE aqueous solutions, for aerogels with a porosity  $P = 98.5\%$  ( $\blacktriangle$ ),  $P = 90\%$  ( $\blacksquare$ ), and  $P = 80\%$  ( $+$ ). The curves are reported in the normalized form, i.e., as  $M_{\text{DCE}}(t)/M_{\text{DCE}}(\infty)$  vs  $t^{1/2}/L$  ( $L$  = sample thickness), where  $M_{\text{DCE}}(\infty)$  refers to the mass of DCE evaluated at equilibrium (i.e.,  $t = \infty$ ).

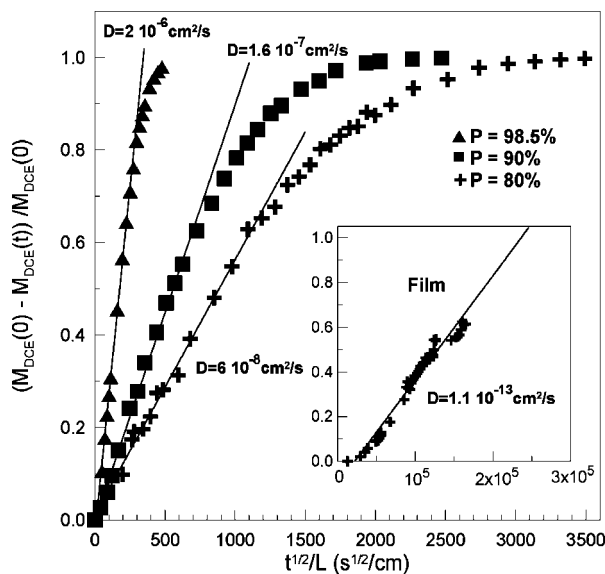


**Figure 5.** Desorption kinetics of DCE at room temperature, after equilibrium sorption uptake from a 100 ppm aqueous solution, for aerogels with a porosity  $P = 98.5\%$  ( $\blacktriangle$ ),  $P = 90\%$  ( $\blacksquare$ ), and  $P = 80\%$  ( $+$ ). The desorption kinetics of a film is reported as inset (data from ref 6d). The curves are reported in the normalized form, i.e., as  $(M_{\text{DCE}}(0) - M_{\text{DCE}}(t))/M_{\text{DCE}}(0)$  vs  $t^{1/2}/L$  ( $L$  = sample thickness), where  $M_{\text{DCE}}(0)$  refers to the mass of DCE evaluated at equilibrium (i.e.,  $t = 0$ ).

Figure 6 shows that the two aerogels for high desorption times present similar desorption kinetics, while for short times, the high-porosity aerogel present an additional faster desorption phenomenon. We have observed by FTIR measurements (see Supporting Information) that the initial fast desorption process, clearly apparent for the high-porosity aerogel, corresponds to loss of water while the subsequent desorption process (being slower and common to both aerogels) corresponds to release of the organic guest from the cocrystalline phase.

The gravimetric results of Figure 6 confirm that  $\delta$ -aerogels of s-PS are able to absorb large amounts of DCE (e.g., up to 7 wt % from 100 ppm solution), independently of their

**Table 2.** Apparent Diffusivity Constants at Room Temperature of DCE in s-PS Samples, Presenting the Nanoporous  $\delta$ -Crystalline Phase, for Absorption from Diluted Aqueous Solutions and Subsequent Desorption in Air

$\delta$ -form samples of s-PS	$D$ [ $\text{cm}^2/\text{s}$ ] (absorption)	$D$ [ $\text{cm}^2/\text{s}$ ] (desorption)
010 oriented film <sup>a</sup>	$6.8 \times 10^{-13}$	$0.3 \times 10^{-13}$
unoriented film <sup>a</sup>	$8.6 \times 10^{-13}$	$1.1 \times 10^{-13}$
( $\bar{2}10$ ) oriented film <sup>a</sup>	$9.9 \times 10^{-13}$	$4.3 \times 10^{-13}$
aerogel, $P = 80\%$	$8.4 \times 10^{-8}$ (100 ppm)	$6.0 \times 10^{-8}$ (100 ppm)
aerogel, $P = 90\%$	$2.3 \times 10^{-8}$ (10 ppm)	$1.6 \times 10^{-7}$ (100 ppm)
	$1.7 \times 10^{-7}$ (100 ppm)	
aerogel, $P = 98.5\%$	$6.6 \times 10^{-6}$ (10 ppm)	$2.0 \times 10^{-6}$ (100 ppm)
	$1.0 \times 10^{-5}$ (100 ppm)	

<sup>a</sup> Data from ref 6d, which refer to sorption of DCE from 50 ppm aqueous solutions into films with a thickness of 30–40  $\mu\text{m}$ .

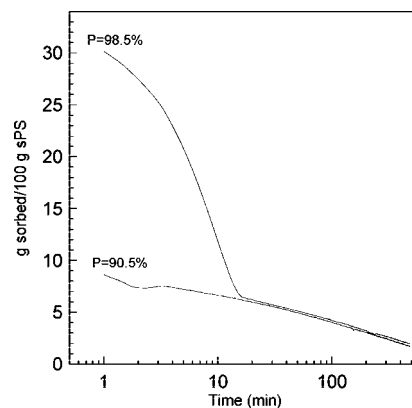


**Figure 6.** Gravimetric desorption kinetics of  $\delta$ -aerogels with porosity  $P = 90.5\%$  and  $P = 98.5\%$ , after equilibrium sorption in 100 ppm aqueous solution of DCE.

porosity. Moreover, Figure 6 shows that the high-porosity aerogel ( $P = 98.5\%$ ) is able to adsorb large amount of water (more than 20 wt %) from the water solution.

In this respect, it is worth adding that analogous sorption experiments from pure water have shown that the water uptake in all the prepared sPS aerogels is negligible, as expected on the basis of the well-established hydrophobic behavior of polystyrene.

Hence, this water adsorption by the amorphous aerogel pores, being induced by the presence of suitable organic solutes, is possibly due to interactions between water molecules and DCE molecules adsorbed on the polymer surface. This water adsorption phenomenon is of course beneficial to the kinetics of the organic guest absorption by the crystalline nanocavities.

### Conclusions

The uptake of nitrogen at 77 K and of VOC from aqueous solutions at room temperature, for a series of aerogel samples with different crystalline forms and porosities, has been investigated.

The low-temperature nitrogen uptake from  $\delta$ -form aerogels is much higher than from other  $\delta$ -form samples and strongly increases with aerogel porosity. These phenomena indicate that nitrogen *absorption* in the crystalline nanocavities is additive with respect to nitrogen *adsorption* from the amorphous porosity.

Gravimetric and FTIR measurements show that the uptake of organic molecules from dilute aqueous solutions is negligible for s-PS aerogels with dense  $\beta$ - and  $\gamma$ -crystalline phases, while it is high for  $\delta$ -form aerogels (e.g., more than 5 wt % from a 1 ppm DCE solution). The VOC sorption is similar to those observed for other  $\delta$ -form samples, and it is independent of aerogel porosity. These results indicate that the organic guest uptake from diluted aqueous solutions occurs essentially only in the crystalline nanocavities. This has been confirmed by a study of conformationally sensitive FTIR peaks of 1,2-dichloroethane molecules adsorbed in s-PS aerogels.

Gravimetric experiments, associated with the FTIR measurements, have also shown that high-porosity  $\delta$ -form

aerogels ( $P > 98\%$ ) also present substantial water *adsorption* from the amorphous porosity. The adsorbed water is released at a much faster kinetics with respect to organic guests, which are instead adsorbed in the crystalline nanocavities. This water adsorption, occurring only from aqueous solutions including organic compounds, is favorable for the kinetics of removal of diluted pollutants from water by s-PS  $\delta$ -aerogels.

Sorption and desorption experiments of DCE guest molecules have shown that the use of  $\delta$ -aerogels results in an apparent increase in the guest diffusivity of several orders of magnitude (up to 7!) with respect to  $\delta$ -form films.

In summary, these findings confirm that  $\delta$ -form s-PS aerogels present high sorption capacity and fast kinetics as well as convenient handling characteristics. Moreover, by increasing their porosity, it is possible to substantially increase their surface area and sorption kinetics. This makes these materials particularly suitable as sorption medium to remove traces of pollutants from water and moist air.

**Acknowledgment.** Financial support of the “Ministero dell’Istruzione, dell’Università e della Ricerca”, and Regione Campania (Legge 5 and Centro di Competenza) is gratefully acknowledged. Mr. A. Avallone is gratefully acknowledged for technical assistance in preparing aerogel samples. Professors P. Ciambelli, G. Mensitieri, P. Musto, E. Reverchon, and V. Venditto are gratefully acknowledged for useful discussions.

**Supporting Information Available:** FTIR spectra collected at different desorption times of a high-porosity aerogel ( $P = 98.5\%$ ) after equilibrium sorption in 100 ppm aqueous solution of DCE. This material is available free of charge via the Internet at <http://pubs.acs.org>.

CM702475A